Investigation of Otto Fuel Explosion Accident

Prepared by:
Darrell D. Barker, P.E.
Quentin A. Baker, P.E.

Wilfred Baker Engineering, Inc.
August 20, 1996

Abstract

An accidental explosion involving a torpedo test vehicle occurred at a test facility in February 1995. The test vehicle was operating in a 3 inch thick pressure vessel when the incident occurred. The pressure vessel failed catastrophically with the resulting high speed fragments causing extensive damage to the reinforced concrete test cell. The 18 inch thick cell walls and roof were completely perforated by the fragments.

An investigation was performed to document the damage and assist the Navy in determining the cause of the accident. This investigation included reconstruction of the pressure vessel and major portions of the test vehicle. Calculations were performed to estimate the source energy necessary to produce the observed damage. These calculations included empirical methods as well as hydrocode simulations. Materials testing was performed on the pressure vessel and concrete elements to determine properties for use in the calculations.

This paper describes a portion of the investigation effort and includes a description of damage, fragment collection procedures, reconstruction efforts, and source energy calculations. Design for new test cells are also discussed.

Introduction

An accidental explosion occurred on February 24, 1995 in the main test cell of Building 179. The accident at Naval Underwater Warfare Center (NUWC) - Newport occurred during an operational test of a MK 48 propulsion system. The pressure vessel in which the test vehicle was being tested fragmented, subsequently causing severe damage to the test cell. Fragment and debris dispersal was limited to the area immediately adjacent to the test cell. Exclusion zones in place for the test operations based on quantity-distance (Q-D) considerations ensured that personnel were not exposed to the debris hazard.

Wilfred Baker Engineering, Inc. was tasked with a portion of the investigation effort which included documenting damage, determining energy of the explosion, and evaluating blast capacity of the test cell. These objectives were met by mapping fragment locations, documenting structural damage, collecting and reconstructing fragments from the test vehicle and pressure vessel, and analyzing fragmentation and blast damage. Explosion energy was estimated through calculation of vessel fragment velocities consistent with penetration through the reinforced concrete walls and roof of the

Report Documentation Page

Form Approved
OMB No. 0704-0188

1. REPORT DATE	2. REPORT TYPE	3. DATES COVERED
20 AUG 1996		**00-00-1996 to 00-00-1996**

4. TITLE AND SUBTITLE	5a. CONTRACT NUMBER
Investigation of Otto Fuel Explosion Accident	5b. GRANT NUMBER
	5c. PROGRAM ELEMENT NUMBER
6. AUTHOR(S)	5d. PROJECT NUMBER
	5e. TASK NUMBER
	5f. WORK UNIT NUMBER
7. PERFORMING ORGANIZATION NAME(S) AND ADDRESS(ES) **Wilfred Baker Engineering, Inc,8700 Crownhill Blvd,San Antonio,TX,78209-1128**	8. PERFORMING ORGANIZATION REPORT NUMBER
9. SPONSORING/MONITORING AGENCY NAME(S) AND ADDRESS(ES)	10. SPONSOR/MONITOR'S ACRONYM(S)
	11. SPONSOR/MONITOR'S REPORT NUMBER(S)

12. DISTRIBUTION/AVAILABILITY STATEMENT
Approved for public release; distribution unlimited

13. SUPPLEMENTARY NOTES
See also ADM000767. Proceedings of the Twenty-Seventh DoD Explosives Safety Seminar Held in Las Vegas, NV on 22-26 August 1996.

14. ABSTRACT
see report

15. SUBJECT TERMS

16. SECURITY CLASSIFICATION OF:			17. LIMITATION OF ABSTRACT	18. NUMBER OF PAGES	19a. NAME OF RESPONSIBLE PERSON
a. REPORT	b. ABSTRACT	c. THIS PAGE			
unclassified	**unclassified**	**unclassified**	**Same as Report (SAR)**	**14**	

cell and limited dispersal. Evaluation of test cell capacity was performed using conventional blast analysis methods.

Description of Damage

The main test cell of Building 179 was constructed of 18 inch thick reinforced concrete walls and roof. Plan dimensions for the cell were 14 ft wide and 34 ft long with a height of 14 ft as shown in Figure 1. This cell was bordered by smaller test cells on two sides. One wall of the structure was designed to vent an explosion and was constructed of angle framing with fiberglass panels.

Damage to the test cell was substantial. Detonation or decomposition of the monopropellant, Otto fuel, created a shock wave which destroyed the 3 inch thick, water-filled containment pressure vessel. Fragments from the vessel traveled radially from the centerline and impacted the north and south walls, roof slab, and floor. The most extensive damage occurred in the roof where approximately 85% of the roof slab was removed. The post accident condition of the roof indicated that reinforcing bars in the roof slab did not develop sufficient anchorage to rupture the reinforcing. Instead, splices located near the edge of the roof slab separated and released large sections of the slab. Vessel fragment impacts on the concrete caused the walls and roof to break into numerous pieces. Most of the concrete debris from the roof fell back into the cell with portions deposited on the roof around the perimeter of the hole. A small percentage of the concrete debris was distributed to the north and the south of the bay out to a distance of about 60 ft. The floor slab was damaged over approximately 40% of the surface with some damage extending near mid-depth. Damage to the cell and distribution of concrete fragments is shown in Figure 2.

Four pieces of the containment vessel were found to have penetrated the roof slab during the accident. One of these fragments weighed approximately 500 lbs with the remaining ranging from 100 to 150 lbs. This finding indicates that the 18 inch thick roof slab was sufficient to prevent perforation of most of the vessel fragments.

The center section of the north wall of the test cell also sustained substantial damage. Most of this wall was completely removed by vessel fragments which produced bond failure of lap splices at the edges of the perforated area. Approximately five vessel fragments perforated this wall. All concrete debris and vessel fragments from the north wall were completely contained within the small concrete cell on the north side of the building.

Damage to the south wall near the center of the explosion source was substantial. This wall section was not completely removed; however, it was damaged to the point of localized failure. There was minimal evidence of fragment impacts on the west rear wall separating the cell from the dynomometer room. The east wall of the cell consisted of an angle frame with fiberglass panels designed to swing open. One side of this panel was thrown approximately 15 ft from the edge of the cell. The south portion of the panel remained attached to the hinge and impacted the frangible wall of the small cubicle to the south of the test cell.

Portions of the pressure vessel were thrown out the front of the bay (east) and came to rest near the west edge of the paved area. These fragments comprised the domed end of the vessel plus sections

of the support frame and rail carrier wheels. The test cell on the south edge of Building 179 was not significantly damaged during the accident. Some fixtures appeared to have been displaced; however, cracking and fragment damage of the north wall was not observed.

Damage to the dynomometer room equipment was substantial. The force of the explosion caused the drive shaft to dislodge the dynomometer and the utility connections. Portions of the masonry wall were also damaged, but no roof damage was observed. Damage outside the test cell was limited to fragment impacts on portable buildings located to the east of Building 179. Minimal blast pressure damage was observed outside of the cell.

The test cell provided adequate protection to personnel by limiting the dispersion of fragments and building debris to the immediate area. The accident underscored the importance of exclusion areas for potentially hazardous operations

Blast and Fragment Damage Documentation

Test Cell Damage

Photographs of the entire accident site, including aerial and ground shots, were made to document the extent of damage and the dispersion of fragments and building debris. Videotape of the test cell and surrounding area was taken to provide additional documentation of the damage. Damage to each of the structural elements of the test cell was also documented with photographs. Damage to the roof and walls of the test cell, which included perforating and nonperforating fragment impacts, was surveyed to document the extent of the damage. Data on penetration depth was also recorded during this survey. Contours for the crater created in the test cell floor slab were produced from grade surveys. A damage map for each surface of the test cell was developed from this information.

Fragment Collection

The site contained numerous fragments dispersed by the accident. An extensive search was then conducted for pieces of the pressure vessel and test vehicle which were mapped and collected. A fragment collection grid was drafted before any fragments were collected. The grid areas were sized and located according to density of fragments visible on the ground directly east of the test cell. In other directions where fragments were less numerous the grid areas were defined by existing features of the site which enabled easy recognition of the area borders. For example, buildings, edge of asphalt lines, etc., were used as area boundaries. After the fragment grid map was finalized, the borders of the grid areas were marked on the ground and fragment collection began.

Debris Collection

During the fragment collection effort, some demolition and debris collection was necessary to allow safe access to all areas in and around the test cell. The roof of the test cell was damaged heavily and required some remediation before any work could be performed safely beneath it. Also, many fragments inside the main cell and adjoining test cells were covered by concrete debris and other structure related debris.

The concrete debris was collectively weighed in each fragment collection grid area in order to produce a contour map of the concrete debris distribution. Concrete debris which remained inside the test cell or any adjacent cell could have originated from the damaged walls and were not weighed or included in the concrete distribution contour map. The weight of concrete from each grid area was converted to a density value of pounds per square foot which was then plotted by distance and direction from the center of the test cell and contour lines were drawn. This was done to determine the distribution of concrete debris from the damaged roof and allow computation of probable initial velocities for the debris.

Pressure Vessel Damage

Reconstruction

The pressure vessel was nominally a 36 inch inside diameter, 24 ft long, 3 inch wall carbon steel vessel. It was constructed using a forged flange ring that was welded to six cylindrical sections. The forward end of the vessel was an elliptical head with a single penetration on centerline. The material specification for the cylindrical sections and domed head was A212 Grade B.

A total of about 135 fragments were recovered for the pressure vessel, of which about 90 were fitted together during the reconstruction. Fragments that were reconstructed represent about 95% of the surface area of the vessel. The vessel was completely reconstructed within the first 13 ft of the vessel from the rear flange, and within the forward most 4 ft long cylindrical section and elliptical head. Inspection of the rupture disk housing revealed that the disk had ruptured.

Fragments from all five of the penetrations in the vessel were collected. It was observed that crack lines did not run through any of these openings. There was no indication that stress concentrations around any of the holes was responsible for a crack origination.

The girth and longitudinal welds for each cylindrical section were examined. The cracks did not follow any of the weld lines with the possible exception of a 13 inch length on the girth weld between the fourth and fifth cylindrical sections. However, this weld was not a source of crack initiation.

The fragment size varied considerably along the length of the vessel as depicted in Figure 3. The smallest fragments were located in a band that began about 16 ft forward of the rear flange and terminated at about 17.5 ft as mentioned above. The fragments were consistently of a small size and were randomly spaced around the circumference. Forward and aft of this section, fragment sizes became noticeably larger. There was a band from about 12 ft to about 16 ft forward of the flange where the fragments were “medium” size. The smallest fragments in this zone were located under each of the two tracks at the bottom of the vessel, with a few larger fragments between the tracks. The largest fragments were located at the top of the vessel.

Aft of the zone, the fragment sizes became very large. The largest single fragment was from the top of the vessel and measured 10.5 ft from the flange to the forward tip. At the flange, it comprised approximately half the vessel circumference.

Fragment Location

Several vessel fragments were traced along the path they followed from the original position to their final resting place after the explosion as shown in Figure 4. The paths followed by the fragments indicate the general direction most vessel fragments traveled after the explosion. The fragments used for this exercise were first located in the reconstructed vessel layout and a path was plotted to the location they were found. A few fragments penetrated the cell walls and were found in adjacent test cells. The paths for these fragments were plotted to the holes in the walls and then to the location where they were found, creating a deflected path for a few of the fragments. One fragment used in this analysis was found on the opposite side of the test cell from its original position indicating a ricochet. One of the larger impact locations on the south wall of the test cell was used in determining its path.

It was concluded from the pressure vessel reconstruction that the explosion was centered in the band of small fragments that was located from 16 to 17.5 ft forward of the rear flange. Given the uniformity of the size of the small fragments around the circumference of the vessel within this band, it was further concluded that the explosion occurred along the centerline of the vessel. The rather significant increase in fragment size either side of the band of small fragments indicates that the preponderance of the explosion energy was released within this band. This did not preclude a small explosion occurring in another part of the vessel before the vessel failed, but it did indicate that the main explosion occurred within the band described above.

Explosion Energy Analysis

Characterization tests on Otto fuel have indicated that the TNT equivalency may be approximately equal to 100% for certain confined configurations of large fuel quantities. This fuel has the potential to detonate when initiated by a sufficient amount of explosive (Reference 1). Under certain environmental conditions, the fuel will decomposition and produce a load which has a lower energy release rate than a detonation. The breakup pattern of the containment vessel indicated that a very fast energy release rate was produced during the explosion. The relatively small size of the fragments in one region of the pressure vessel was indicative of a detonation event.

Following initiation of the fuel mass within the forward portion of the test vehicle, a high energy, short duration shock wave emanated from the detonation and impacted the walls of the water-filled containment vessel. This shock wave reverberated within the vessel and the reflections created an additional load on the vessel walls. Shock loads produced tensile stresses within the vessel wall which exceeded the ultimate strength of the material. This caused the vessel to rupture sending high energy steel fragments radially outward from the explosion.

The vessel fragments impacted the surrounding reinforced concrete elements of the test cell. The impacts imparted impulsive loads on these elements, producing flexural and shear stresses within the concrete. Because the reinforcing in the concrete was not well anchored, these elements were not able to resist the fragment impulse loads in flexure. A lack of adequate shear reinforcing in these members produced shear failure at the supports.

The only other resistance to penetration and perforation of fragments was the shear capacity of the concrete. A portion of the fragment kinetic energy was absorbed by the concrete during breakup as strain energy and kinetic energy. The majority of the fragments were arrested, transferring all of their kinetic energy into the concrete creating debris.

Most of the concrete debris was launched at an angle between 0^0 and 15^0 from the normal to the plane of the roof slab. This dispersal pattern is quite common for elements which are completely overwhelmed by a blast load. As a result, most of the concrete debris fell back into the cell or very close to the perimeter of the roof slab.

Fragment throw documented during the forensic investigation was used to determine an initial velocity for the pieces of the vessel after perforation of the roof slab. A range of launch angles and initial velocities were developed for each of the vessel fragments which were recovered exterior to the cell and which had penetrated the roof slab. Concrete debris throw was also used to develop a range of initial velocities and launch angles which would produce the debris dispersion observed. The mass and initial velocity of the concrete debris and the vessel fragments following penetration were used to compute a kinetic energy of exiting fragments. Using conservation of energy, it was possible to predict initial fragment velocity prior to striking the roof slab by balancing the impact kinetic energy with the exiting fragment and debris kinetic energy. Because of the low flexure and shear capacities of the roof slab, it was assumed that no energy was absorbed through flexural response of the slab. The energy absorbed during perforation of the vessel fragments was computed using methods developed by Ross and Rosengren (Reference 2) for impulsive loads.

The site investigation revealed that there was not a significant amount of reinforcing steel which appeared to be sheared by fragments or appreciably strained in tension. This indicated that the reinforcing did not work to absorb the fragment energy. So the determination of critical velocity for the steel vessel fragments was based solely on the concrete tension capacity.

The results of compression tests on specimens taken from the site indicated a concrete compressive capacity of 7,821 psi. This is significantly higher than the specified minimum strength of 3,000 psi. Typically, the concrete tension capacity is 10% to 15% of the compressive capacity. Based on this relationship, the tension capacity was expected to be approximately 780 psi. A pull test was also conducted on the concrete samples in which a tension capacity of only 150 psi was measured. It is likely that the specimen used for the tensile test sustained microcracking during the explosion and thus yielded low tensile strength in the static pull tests. Values for critical velocity were calculated, for both of the tension capacities given.

A critical velocity of 113 ft/sec was calculated for the case where the tension capacity is approximately 150 psi. A critical velocity of 260 ft/sec was calculated for the 780 psi tensile capacity case. These two values were used to create a lower and upper bound for the amount of energy that was absorbed by the concrete during perforation by the steel fragments.

With the kinetic energy of the vessel fragments prior to impact known, an initial striking velocity was computed. It was assumed that there was a negligible decrease in the fragment velocity during flight from the pressure vessel to impact with the concrete surface.

Two separate methods were then used to compute a source energy which would produce the predicted initial velocities. The first was an empirically based procedure, termed the Gurney method described in TM 5-1300 (Reference 3). This method was developed for prediction of fragment velocities for cased explosives. The Gurney method is applicable to a cylindrical charge surrounded by liquid and a steel case. Weight of the water was added to the weight of the pressure vessel in accordance with recommended application of this method. An equivalent weight of TNT was then computed by calculating the charge weight required to produce the initial striking velocities described above.

One major difference was noted between the Gurney method assumptions and the actual conditions present in the test vehicle explosion. The charge is considered to be a constant cross section throughout the case in the Gurney method. The actual explosion was postulated to have occurred in one section of the test vehicle. Thus, the explosion was not constant along the length of the containment vessel. Empirical data from Whitney, et. al., (Reference 4) closely resembled the explosive charge separated by a fluid, similar to the steel containment vessel and the test vehicle, but on a smaller scale. This data indicated that in the midsection of the vessel, the ratio of calculated to measured initial velocity was an average of 1.75. This ratio was applied as a velocity correction factor to account for the differences between the test vehicle explosion and the theoretical assumptions in the Gurney method. Using the adjusted initial velocity of the fragment, a charge weight was determined.

The second method involved the use of a hydrodynamic code (hydrocode). This code AUTODYN (Reference 5) numerically models the physical processes which occur during an explosion event. The program tracks the travel of the shock wave following the explosion and predicts response of the containment vessel. A hydrocode is a finite element-like program in that the model is gridded into zones. The equations of state and thermodynamic properties of the materials are used in the analysis to describe their behavior of under hydrodynamic loads. This allows a hydrocode to analyze transient phenomena such as the detonation front of explosives and the propagation of shock waves in solids, liquids, and gases. The equations of state properties allow the material to fail at a specified strain or stress, and to change phases under extremely high loadings. The code was allowed to run until such time as an initial velocity for the vessel fragment was predicted. This procedure was followed for four source energies to establish a relationship between source energy and initial fragment velocity. These results were then compared with the empirical calculation methods.

The test vehicle housing was neglected as it was very thin. The instrumented nose cone of the test vehicle was modeled as 1 inch thick aluminum. It was assumed that since the air on the inside of the instrumented nose cone was at atmospheric pressure, as opposed to the hydrostatic pressure inside the pressure vessel, its effects were negligible. Therefore, the interior of the nose cone was assumed to be void. The aft and forward afterbody fuel tanks were modeled as being completely full of water at equilibrium pressure. The afterbody was modeled as being completely full of air at equilibrium pressure. The fuel in the forward section was modeled as TNT. It was assumed that ignition occurred at the centerline and the shock wave traveled outward from the centerline. The total volume of fuel used in the model was varied to established a relationship between fuel volume and initial fragment velocity. The aluminum bulkhead of the instrumented nose cone section deflected some of the shock energy toward the aft end of the test vehicle. The initial shock wave for a charge

weight of 131 pounds TNT was predicted to have a peak pressure of 555,000 psi (3.83×10^6 kPa) and a duration of 0.1 ms at a location on the pressure vessel wall opposite the charge.

The shell of the pressure vessel was initially modeled using the equation of state of iron. A yield stress of 38,000 psi and an ultimate stress of 70,000 psi were used. The plastic modulus was computed such that 21% strain occurred at ultimate stress (rupture). The initial velocity of the shell was predicted to be 275 ft/s (84 m/s) for the 131 lb load. At a time of 1.04 ms after initiation, the shell was predicted to fail. A fracture mechanics approach was not incorporated into the hydrocode model. Thus, although the shell of the pressure vessel is predicted to fail under high stress loadings, the fragment size may not be representative of an experimental model or an accident. The initial fragment velocity, however, was expected to be representative.

The source energy predicted by the hydrocode modeling was equivalent to approximately 100 lbs of TNT. Using a 100% TNT equivalency, this would yield a weight of 100 lbs or Otto fuel participating in the detonation. This is close to the weight of the fuel in the forward section which was approximately 140 lbs. From this we concluded that much of the fuel in the forward section participated in the explosion and was effective in producing the computed initial velocity of the vessel fragments. This would also indicate that the detonation of the fuel in the bottom of the forward fuel tank did not influence the initial velocity of fragments at the top of the vessel. The fragmentation pattern at the bottom of the vessel in the forward fuel tank region was indicative of a detonation; however, the top portion of the vessel in this area was broken into larger pieces. We concluded that most of the energy from the fuel in the bottom of the forward fuel tank was directed downward, contributing to the crater.

The effect of the water and pressure vessel is to limit the shock wave emanating from the ruptured vessel. This results from the shock wave being transferred into kinetic energy of the water and vessel fragments. A gas pressure pulse is produced by the detonating Otto fuel; however, the large heat sink provided by the mass of the water effectively limits gas temperature rise, thus significantly reducing the long term gas pressure loads. This same effect is anticipated for a configuration with the maximum fuel load; however, the fuel to water volume ratio would be much higher for that situation and the water may not be as efficient in reducing or eliminating the gas impulse. This could result in introduction of gas pressure loads within the bay. Neither of these phenomena is expected to significantly alter the predicted range of hazardous fragments and debris.

The effective source energy was computed independently by the empirical methods and the hydrocode calculations described above. The empirical methods produced an equivalent energy of 75 lbs of TNT while the hydrocode predicted an equivalent source energy of 100 lbs TNT. These analyses showed reasonable agreement for the effective source energy. The hydrocode analysis predicted vessel breakup in the area directly across from the charge which was also observed in the zone of small fragments from the vessel wall in the location of the forward section.

Cell Design Considerations

The conventional means for designing a test cell would be to treat the design basis accident (DBA) charge weight as an unconfined explosives charge. Due to the large DBA charge weight for test cells of this type, it is not normally feasible to design a cell to contain blast pressures produced by

an unconfined charge Instead, the cell structural elements can be permitted to be severely damaged due to blast loads while maintaining a safe siting distance for building debris. An eyebrow and mobile barricade may be necessary to restrict the flight of cylinder and head fragments from the pressure vessel toward the entrance to the cell.

Testing in a thick walled pressure vessel significantly changes the blast hazard. Instead of shock loads applied to the walls, fragment impact becomes the primary design consideration. The cell must prevent escape of primary fragments to meet fragment protection criteria.

Analysis methods used during the investigation can be used to design structural elements for new test cells. Hydrocode and hand calculations were in good agreement indicating that the latter can be used determine initial sizing and verified by the more complex hydrocode analysis.

To increase the fragment impact capacity of concrete walls, substantial reinforcing, well anchored into walls, must be provided. The reinforcing picks up significant load in membrane response and provides greater shear capacity than the concrete. This type of response was not seen in the explosion accident due to insufficient development of reinforcing lap splices.

Conclusions

The test cell involved in the explosion accident provided adequate protection to personnel. The test cell sustained severe damage due to an explosion in a torpedo propulsion system located in a water-filled pressure vessel. The predominant damage mechanism was fragment impact following rupture of the pressure vessel. Pressure vessel fragments perforated 18 inch reinforced concrete cell walls and roof, and cratered the cell floor although airblast damage was negligible. Roof damage was unusually heavy due to inadequate reinforcement anchorage at splices. Nonetheless, the roof arrested the throw of all but four fragments.

The energy released during the explosion was estimated by two independent methods to be between 75 and 100 lbs TNT equivalent. Pressure vessel fragment velocities were predicted based on wall and roof damage. The Gurney method and a hydrocode anlaysis were independently used to predict the energy, and were in reasonably good agreement.

References

1. “Otto Fuel II Safety, Storage, and Handling,” NAVSEA OP-3368, Sixth Revision, Technical Manual, Department of the Navy, Sea Systems Command, October 1, 1976.

2. Ross, Allen C., and Paul L. Rosengren Jr., “Expedient Nonlinear Dynamic Analysis of Reinforced Concrete Structures,” Proceedings of Second Symposium on the Interaction of Non-Nuclear Munitions with Structures, Panama City Beach, Florida, April 15-18, 1985.

3. Departments of the Army, the Navy and the Air Force, "Structures to Resist the Effects of Accidental Explosions," Department of the Army Technical Manual TM 5-1300, Department of the Navy Publication NAVFAC P-397, Department of the Air Force Manual AFM 88-22, November 1990.

4. Whitney, M. G., G. J. Frisenhahn, W. E. Baker, and L. M. Vargas, “A Manual to Predict Blast and Fragment Loadings from Accidental Explosions of Chemical Munitions inside an Explosion Containment Structure,” under Contract No. DACA87-81-C-0099, SwRI-6714, prepared for U.S. Army Toxic and Hazardous Materials Agency and U.S. Army Corps of Engineers, Huntsville Division, April 1983.

5. "AUTODYN Software for Non-Linear Dynamics Users Manual, Version 2.1," Century Dynamics Incorporated, Oakland, CA, 1989.

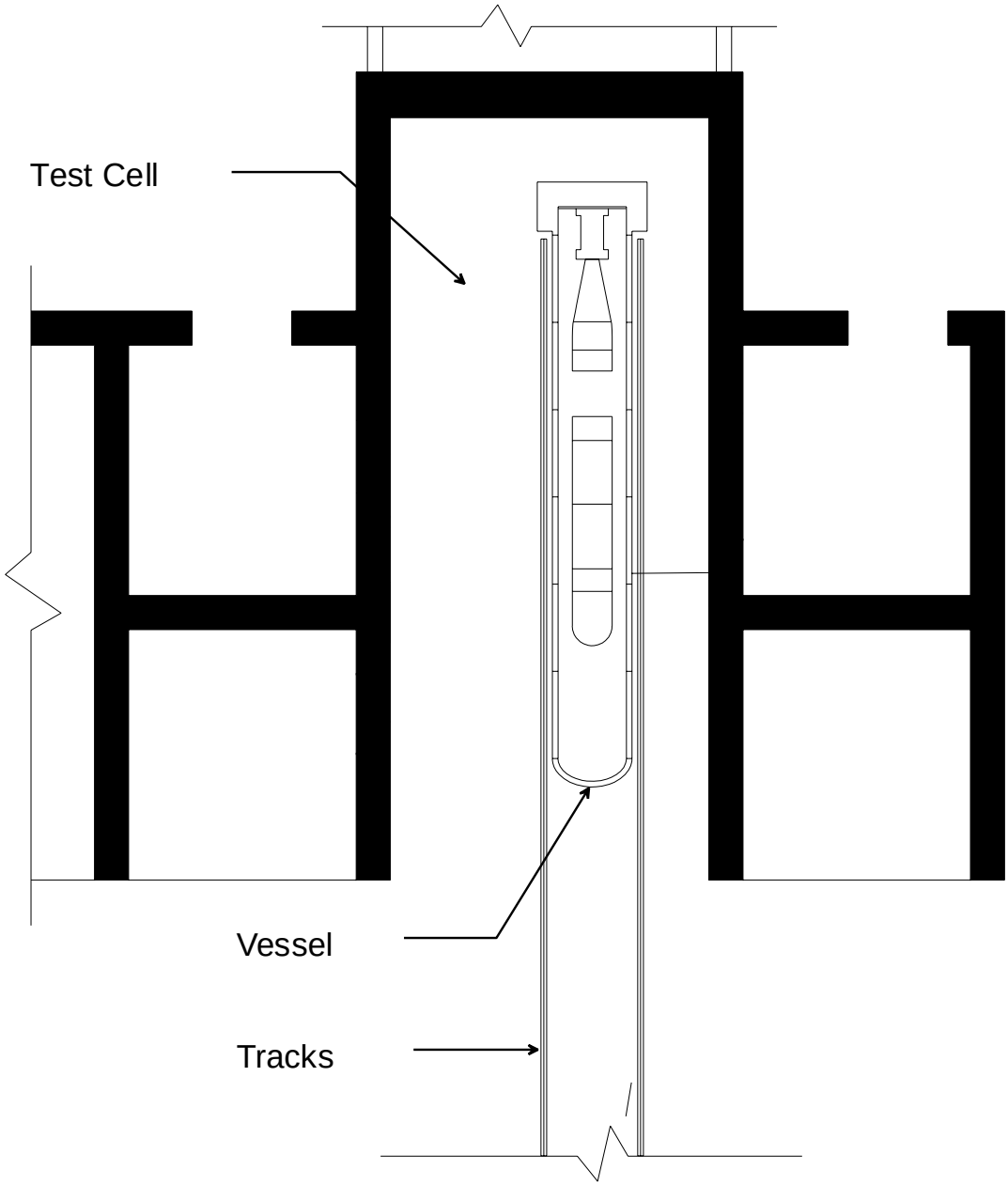

Figure 1. Floor Plan of Test Cell

CONCRETE RUBBLE DISTRIBUTION CONTOURS

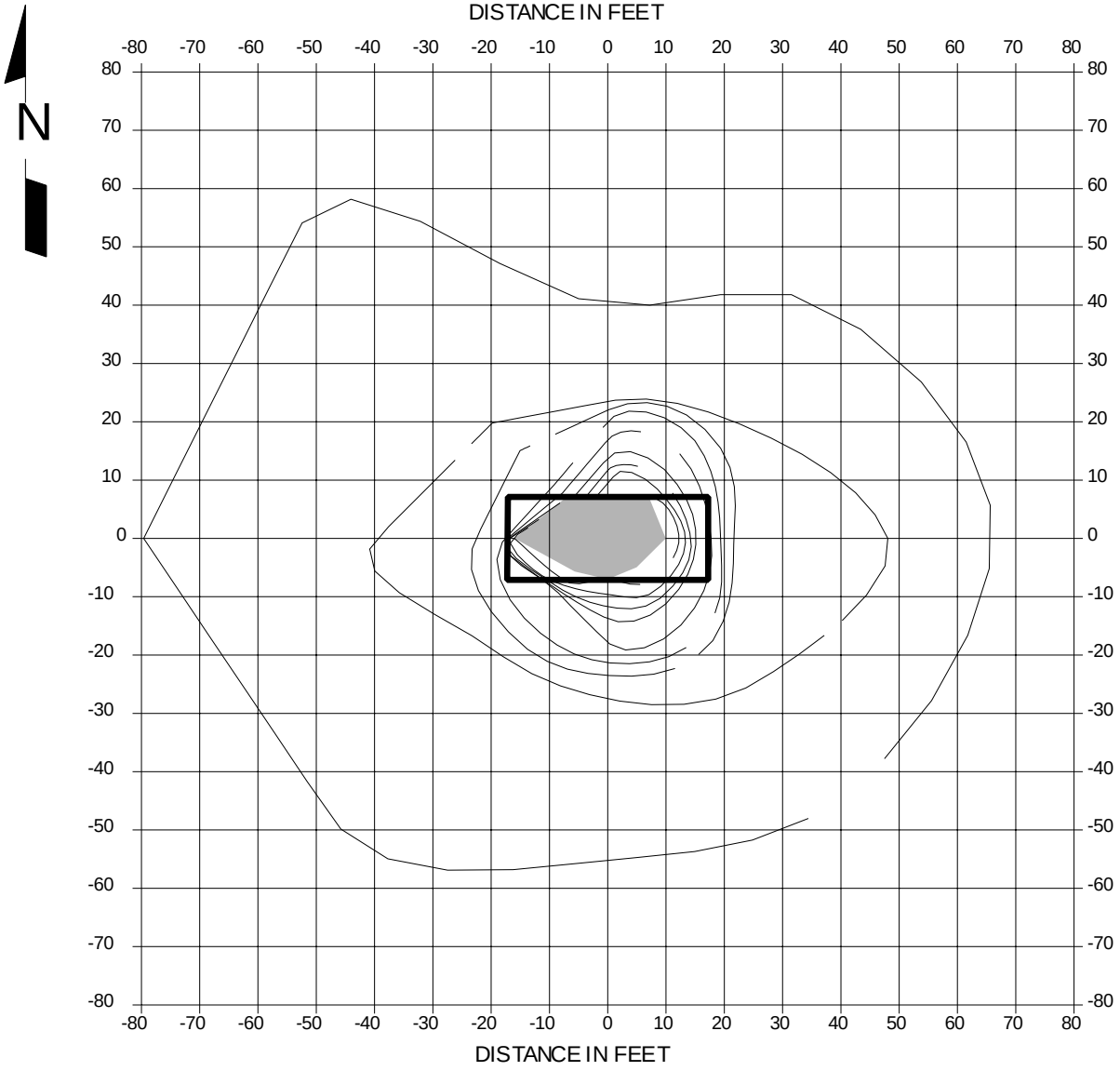

Figure 2. Concrete Debris

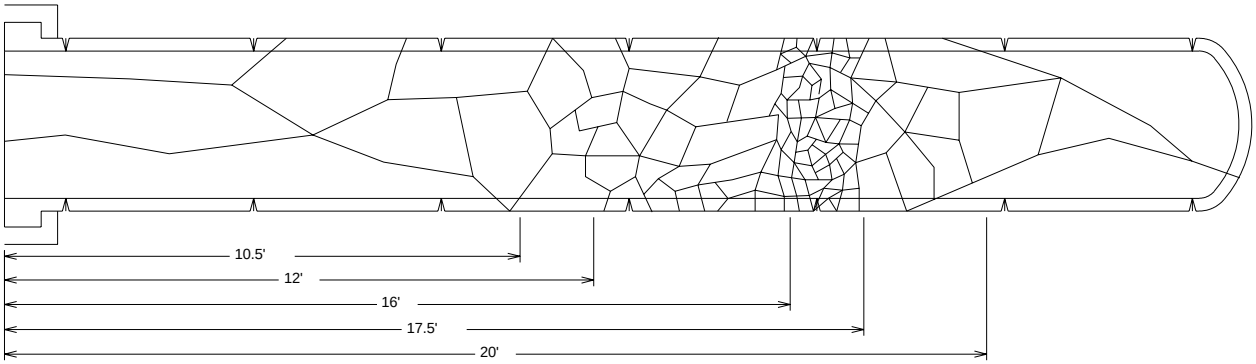

Figure 3. Pressure Vessel Fragmentation

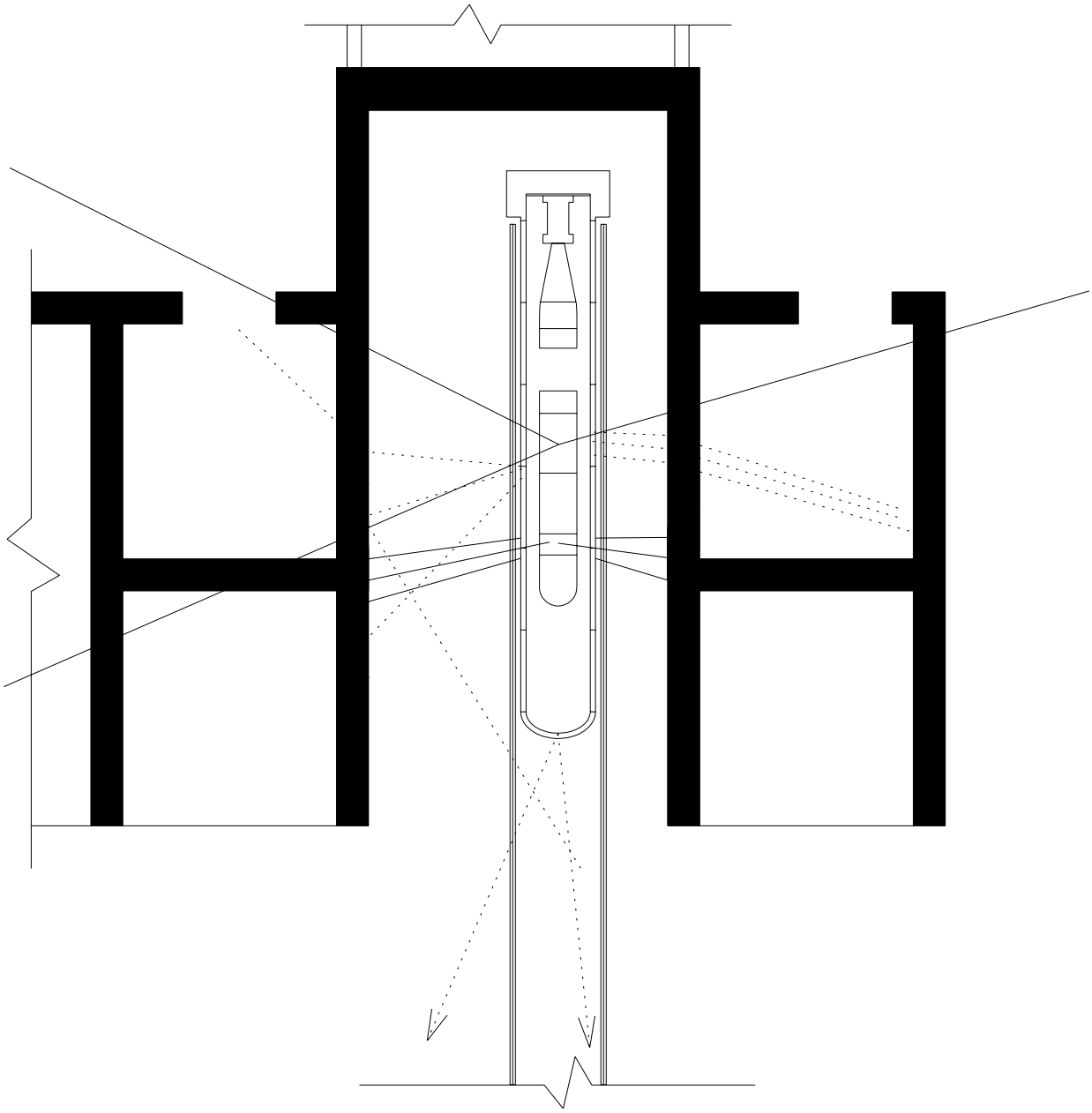

Figure 4. Vessel Fragment Trajectories